

EMISSION OF RADIATION FROM MODEL HYDROGEN CHROMOSPHERES

By J. T. JEFFERIES*

[*Manuscript received October 8, 1952*]

Summary

On the basis of earlier work of Giovanelli (1949), the characteristics of the radiation fields of $H\alpha$, $L\alpha$, $L\beta$, and the Lyman continuum have been calculated for model solar atmospheres consisting of a photosphere and an overlying chromosphere which scatters coherently, and which is isothermal at one of a number of kinetic temperatures in the range 1×10^4 to 2.5×10^5 °K.

The computed central intensities (of $H\alpha$) suggest that the kinetic temperature of those regions responsible for the observed solar $H\alpha$ radiation lies somewhere in the range up to about 3.5×10^4 °K. The best agreement with observation, for those temperatures considered, is obtained for 2.5×10^4 °K., with an electron concentration 2×10^{11} per cm^3 at the base of the chromosphere. Too much reliance should not be placed on this result, for the obvious non-uniformity of the solar chromosphere and its effect on the hydrogen lines has not been taken into account.

The effective black-body temperature for the centres of the $L\alpha$ and $L\beta$ lines and for the Lyman series limit have been calculated; the results indicate that the intensities in each case pass through a maximum at a kinetic temperature about 5×10^4 °K. The half-widths of $L\alpha$ and $L\beta$ show a steady decrease with increasing temperature up to 5×10^4 °K.; for higher temperatures the half-width increases.

The contours of $L\alpha$ and $H\alpha$ have also been computed on the basis of a simple model of non-coherent scattering in which the absorbed radiation is redistributed over a Doppler profile; the results indicate that the type of scattering is unimportant for $H\alpha$, but may considerably modify the profiles of the Lyman lines.

I. INTRODUCTION

The discovery that the temperature in the Sun's atmosphere increases outwards has stimulated studies of the emission of radiation from hot atmospheres, such, for example, as those of Thomas (1948, 1949), Giovanelli (1949), and Miyamoto (1951*a*, 1951*b*). There is considerable uncertainty, however, as to the temperature distribution in the chromosphere, and to assist studies on this subject, and on the temperatures of disturbed solar regions such as flares and prominences, computations are given here of the radiation emitted by model hydrogen chromospheres over a temperature range 2.5×10^5 to 10^4 °K. Below 10^4 °K. collisions between neutral atoms become relatively important, but as there are no data for the excitation cross sections for these collisions, it has not been possible to extend the calculations to lower temperatures.

Investigations by Thomas (1948, 1949) and Giovanelli (1949) on the intensity of Lyman and Balmer radiation in the solar chromosphere, the former assuming a temperature of 35,000 °K., the latter 25,000 °K., have yielded results in

* Division of Physics, C.S.I.R.O., University Grounds, Sydney.

substantial agreement. The methods adopted by the two authors were rather similar, and involved calculating the equilibrium populations established in a hydrogen atmosphere when transitions between atomic states take place as a result of electron collision or the emission or absorption of radiation. Using an equation of radiative transfer, atomic populations and radiation intensities were obtained.

More recently Miyamoto (1951*a*, 1951*b*) has dealt with the excitation of hydrogen and helium in a 30,000 °K. chromosphere. The results obtained for hydrogen are generally in quantitative agreement with those obtained here.

The present method follows closely that of Giovanelli, although improved collision cross sections have been used. The distribution of intensity in the Lyman continuous spectrum and the profiles of $L\alpha$, $L\beta$, and $H\alpha$ are obtained for chromospheres having a scale height either defined by the observed chromospheric electron gradient, or appropriate to hydrostatic equilibrium. Electron concentrations assumed for the base of the chromosphere range in general from 10^{11} to 10^{12} cm.⁻³. Results are obtained first for an atmosphere which scatters coherently; non-coherent scattering is considered in Section IX.

II. LIST OF PRINCIPAL SYMBOLS

The more frequently occurring symbols are as follows:

- T , kinetic temperature,
- z , vertical height above the base of the atmosphere,
- ε_ν , α_ν , "true" emission and absorption coefficients for radiation of frequency ν ,
- B_ν , defined as E_ν/α_ν , E_ν being the total emission coefficient,
- λ_ν , λ'_ν , scattering parameters in the chromosphere and photosphere respectively,
- J_ν , total monochromatic intensity,
- N_l , concentration of hydrogen atoms in the l th substate,
- N_e , N_+ , electron and proton concentrations,
- N_0 , N_e at the base,
- β , electron density gradient in $N_e = N_0 \exp(-\beta z)$,
- $\Lambda_\alpha N_{11}$, rate of absorption of $L\alpha$ radiation per unit volume—similar symbols are used for $L\beta$ and Lyman continuum absorption,
- τ_ν , optical depth for the appropriate radiation,
- τ_1 , τ_1° , values of τ at the base of the atmosphere; at an arbitrary frequency and at the centre of the line (or series limit) respectively.

III. THE EQUILIBRIUM EQUATIONS

The outward diffusion of radiation from an atmosphere which scatters coherently is given by the approximate relation (see Giovanelli 1949)

$$J_\nu = 4\pi\varepsilon_\nu/\alpha_\nu\lambda_\nu + a_\nu \exp(\sqrt{3\lambda_\nu\tau_\nu}) + b_\nu \exp(-\sqrt{3\lambda_\nu\tau_\nu}), \quad \dots (1)$$

where J_ν is the total intensity of the radiation; ε_ν and α_ν are respectively the emission and absorption coefficients; λ_ν is a scattering parameter, and is the probability that an atom which undergoes an upward transition under the

influence of radiation will be ionized, or return to the ground state by some process not involving the emission of radiation of frequency ν ; and τ_ν is the optical depth defined by $\tau_\nu = \int_\infty^z \alpha_\nu dz$. This solution of the equation of radiative transfer assumes that λ is constant and ϵ/α is either constant or varies linearly with optical depth. To satisfy these restrictions and simplify the calculations we consider the radiation emitted by an atmosphere of uniform electron concentration and thickness equal to the scale height.

The values of ϵ , α , and λ depend on the populations of the various atomic states and on the kinetic temperature of the atoms, which we assume equal to the electron temperature.

The populations may be obtained from the condition that, at equilibrium, the rate at which atoms arrive in any quantum state is equal to the rate at which they leave. This may be expressed by the following general equation for the j th substate :

$$\begin{aligned} \sum_l [A_{lj} + \beta_{lj} N_e + I(\nu_{lj})] N_l + \gamma_j N_e^2 + \delta_j N_e^3 \\ = \sum_k [A'_{jk} + \beta'_{jk} N_e + I'(\nu_{lk}) + I'(\nu_{ji}) + \epsilon_{ji} N_e] N_j, \dots \dots (2) \end{aligned}$$

where N_l and N_j are respectively the concentrations of atoms in the l and j substates; N_e is the electron concentration, assumed equal to the proton concentration; $A_{lj} N_l$ is the rate of the spontaneous atomic transition $l \rightarrow j$; $\beta_{lj} N_e N_l$ is the rate of the collision excitation or de-excitation for the transition $l \rightarrow j$, and $I(\nu_{lj}) N_l$ is the rate of the same transition under the influence of radiation. The terms on the right of equation (2) are the corresponding transition rates for processes which remove atoms from the j substate. The last two terms on the left of equation (2) represent the rates of spontaneous and three-body recombination; corresponding terms on the right represent the rates of ionization from the j substate due to absorption of radiation and to electron collision respectively. The rate of the transition $l \rightarrow j$ induced by radiation, denoted by $I(\nu_{lj}) N_l$, is given by

$$I(\nu_{lj}) N_l = \int_0^\infty \frac{J_\nu \alpha_\nu d\nu}{h\nu}.$$

The set of simultaneous equations represented by (1) and (2) cannot be solved exactly. Following Giovanelli (1949) we shall restrict consideration to the $1S$, $2S$, $2P$, $3S$, $3P$, $3D$, and ionized states, and in equations (2) put the intensities of H α and of the Balmer and Paschen continua in the chromosphere equal to those in a black body at 5000 °K., assumptions which do not greatly influence the results obtained.

IV. THE TRANSITION RATES

The rates of radiative transition between two substates of the hydrogen atom, i.e. the A_{lj} 's in equation (2), are well known (see, e.g. Unsold 1938).

The terms β_{lj} and β'_{jk} , which represent collision excitations, may be calculated from the appropriate excitation cross sections as functions of the energy of the exciting electrons. Values of the cross sections for excitation from

the $1S$ and $2P$ states for a number of energies, calculated on the assumption of Born's approximation, were kindly made available by Dr. D. R. Bates, of University College, London. Some of these have subsequently been published (Bates *et al.* 1950).

TABLE 1
RATES OF COLLISION EXCITATION
($10^{-9}N_pN_e$ cm. $^{-3}$ sec. $^{-1}$)

T (°K.)	$1S \rightarrow 2S$	$1S \rightarrow 2P$	$1S \rightarrow 3S$	$1S \rightarrow 3P$	$1S \rightarrow 3D$	$2P \rightarrow 3S$	$2P \rightarrow 3P$	$2P \rightarrow 3D$
1.0×10^4	1.08×10^{-4}	3.82×10^{-4}	2.51×10^{-5}	9.14×10^{-6}	9.90×10^{-7}	18.3	27.4	191
1.5×10^4	6.01×10^{-5}	2.21×10^{-3}	2.86×10^{-4}	1.08×10^{-3}	1.16×10^{-4}	35.3	53.7	417
2.5×10^4	1.46×10^{-1}	5.83×10^{-1}	1.28×10^{-2}	5.10×10^{-2}	5.40×10^{-3}	56.9	85.6	773
5.0×10^4	1.50	7.06	2.01×10^{-1}	8.90×10^{-1}	9.14×10^{-2}	77.6	107	1210
1.0×10^5	4.40	25.4	7.26×10^{-1}	3.83	3.69×10^{-1}	86.0	101	1450
2.5×10^5	6.42	46.8	1.20	7.64	6.76×10^{-1}	80.0	74.4	1385

The rates of electron collision excitation have been found from these values by numerical integration assuming a Maxwellian energy distribution for the electrons at an electron temperature T , results being given in Table 1. Rates of collision ionization and spontaneous recombination are given in Tables 2 and 3.

TABLE 2
RATES OF COLLISION IONIZATION
($10^{-7}N_pN_e$ cm. $^{-3}$ sec. $^{-1}$)

T (°K.)	$1S \rightarrow i$	$2S, 2P \rightarrow i$	$3S, 3P, 3D \rightarrow i$
1.0×10^4	6.41×10^{-8}	8.70×10^{-2}	2.86
1.5×10^4	1.38×10^{-5}	3.83×10^{-1}	5.40
2.5×10^4	1.09×10^{-3}	1.15	8.49
5.0×10^4	2.86×10^{-2}	2.50	1.11×10
1.0×10^5	1.46×10^{-1}	3.17	1.13×10
2.5×10^5	3.68×10^{-1}	3.48	9.27

It is worth noting that because of corresponding changes in the rates of superelastic collisions, uncertainties in cross-section data have in many cases little effect on the computed populations and, therefore, on the emergent radiation.

Inelastic collisions resulting in transitions between states of very small energy separation as, for example, $2S \rightarrow 2P$ are of some interest. Purcell (1952) has recently calculated the cross section of this transition using an impact parameter method finding that proton collisions are considerably more important than electron collisions, the effective cross section being of the order of $10^7 \pi a_0^2$. Such a high cross section would greatly simplify our calculations since the $2S$ and $2P$ states would be populated in the ratio of their statistical weights; similar

conditions would presumably apply in other fine structure states. Because it still seems uncertain, however, whether cross sections computed in the above way yield reliable results for states of very small energy difference, we have chosen to neglect $2S \rightarrow 2P$ transitions. From results obtained here, it would appear that this type of transition will have little effect, in any case, except at the higher temperatures where the $2P$ and $2S$ populations are markedly different.

TABLE 3
RATES OF SPONTANEOUS RECOMBINATION
($10^{-15}N_e^2 \text{ cm.}^{-3} \text{ sec.}^{-1}$)

T (°K.)	$i \rightarrow 1S$	$i \rightarrow 2S$	$i \rightarrow 3S$
1.0×10^4	2.07×10^2	2.15×10	5.20
1.5×10^4	1.56×10^2	1.60×10	3.77
2.5×10^4	1.14×10^2	1.11×10	2.52
5.0×10^4	7.30×10	6.36	1.31
1.0×10^5	4.51×10	3.41	6.68×10^{-1}
2.5×10^5	2.10×10	1.36	2.44×10^{-1}

However, the emergent $H\alpha$ intensity is unlikely to be significantly affected, even at these temperatures, because of the small optical depth ; the $L\alpha$ intensity computed here may be slightly low.

V. THE POPULATION OF THE BASE STATE

In a model chromosphere at 25,000 °K., the ratios of the $2P$ and $3P$ populations to that of the ground state are effectively maintained by the absorption and re-emission of Lyman line radiation (Giovanelli 1949) ; i.e. the rates of radiative excitation $\Lambda_\alpha N_1$ and $\Lambda_\beta N_1$ defined by

$$\Lambda_\alpha N_1 = \int J_{\nu\alpha} d\nu / h\nu \text{ and } \Lambda_\beta N_1 = \int J_{\nu\beta} d\nu / h\nu$$

may be respectively equated to $A_{2P,1S} N_{2P}$ and $A_{3P,1S} N_{3P}$, where $A_{j,l}$ is the appropriate spontaneous transition probability. The same results apply to the cases considered here, provided the atmosphere is optically thick to the Lyman line radiations. In this case the total intensities of $L\alpha$ and $L\beta$ inside the chromosphere will be given by $J = 4\pi\epsilon / \alpha\lambda$.

We now evaluate N_1 on the assumption that this relation holds (in the chromosphere) for all electron temperatures ; this assumption will be shown to break down for the higher temperatures, for which a different procedure is required.

For any given temperature, it may then be shown (Giovanelli 1949) that

$$N_1 = \frac{AN_e^2}{\Lambda_c + BN_e} \dots\dots\dots (3)$$

to within a factor less than 2 over the range of N_e from 10^{10} to 10^{12} cm.^{-3} , $\Lambda_c N_1$ being the rate of photoelectric ionization from the ground state per unit volume,

and A and B numerical constants obtained directly from the equilibrium equations. Value of BN_e are shown in Table 6. If Λ_c is neglected in comparison with BN_e , a procedure whose validity is discussed later, the approximate values of N_1 shown in Table 4 are obtained.

TABLE 4
BASE STATE POPULATIONS : FIRST APPROXIMATION
(SEE TEXT)

T (°K.)	N_1 (cm. ⁻³)
1.0×10^4	$6.86 \times 10^{-1} N_e$
1.5×10^4	$8.78 \times 10^{-2} N_e$
2.5×10^4	$2.09 \times 10^{-4} N_e$
5.0×10^4	$8.78 \times 10^{-6} N_e$
1.0×10^5	$1.28 \times 10^{-6} N_e$
2.5×10^5	$2.63 \times 10^{-7} N_e$

The total optical depth of the chromosphere at the centres of the Lyman lines and at the Lyman series limit may readily be calculated, using the approximate base state populations given in Table 4, from the relation

$$\tau_1^0 = - \int_0^\infty \alpha_{v_0} dz, \dots\dots\dots (4)$$

where

$$\begin{aligned} \alpha_{v_0} &= 2.83 \times 10^{29} N_1 / v_0^3 \quad \text{per cm. for Lyman series limit,} \\ &= 6.02 \times 10^{29} N_1 / \sqrt{T} \quad \text{per cm. for the centre of } L\alpha, \end{aligned}$$

and

$$= 9.66 \times 10^{-13} N_1 / \sqrt{T} \quad \text{per cm. for the centre of } L\beta.$$

Values of the optical depth in the Lyman continuum and of the quantities $\sqrt{3\lambda}\tau_1^0$ for $L\alpha$ and $L\beta$ are shown in Table 5 for $N_0 = 5 \times 10^{11}$ cm.⁻³, $\beta = 6 \times 10^{-9}$ cm.⁻¹, N_0 being the electron concentration at the base of the chromosphere, and β the electron gradient.

TABLE 5
OPTICAL DEPTH OF HYPOTHETICAL CHROMOSPHERES FOR LYMAN RADIATION (SEE TEXT)

T (°K.)	$\sqrt{3\lambda}\tau_1^0(L\alpha)$	$\sqrt{3\lambda}\tau_1^0(L\beta)$	τ_1^0 (Lyman Limit)
1.0×10^4	5.85×10^4	9.90×10^4	4.53×10^2
1.5×10^4	7.30×10^3	1.23×10^3	5.82
2.5×10^4	1.84×10	2.76×10	1.40×10^{-1}
5.0×10^4	6.65×10^{-1}	9.70×10^{-1}	5.78×10^{-2}
1.0×10^5	7.32×10^{-2}	8.51×10^{-2}	8.45×10^{-4}
2.5×10^5	9.38×10^{-3}	1.18×10^{-2}	1.73×10^{-4}

It can be seen that the optical depth of the chromosphere is appreciable in the Lyman continuum, for temperatures of 1.5×10^4 °K. or less, and may be small for the Lyman lines when the temperature is 5×10^4 °K. or more, depending on the value of N_1 . We shall now reconsider the values of N_1 in such cases.

(a) *Effect of the Lyman Continuum*

Neglecting reflection at the base of the chromosphere, the total monochromatic intensity in the Lyman continuum, J_ν , at the top of the chromosphere is given by the relation (see Giovanelli 1949, equation (73)) :

$$J_\nu = \pi G \beta H^{-2} [1 - (1+a) \exp(-a) - a^2 \text{Ei}(-a)], \quad \dots (5)$$

where

$$\begin{aligned} G &= 1.72 \times 10^{-33} T^{-3/2} \exp [(E_1^i - h\nu)/kT], \\ H &= 2.83 \times 10^{29} N_1 / N_e \nu^3, \\ a &= N_o H \beta^{-1}, \end{aligned}$$

and

$$-\text{Ei}(-a) = \int_a^\infty [\exp(-x)/x] dx.$$

E_1^i is the ionization potential and the other symbols have their usual meanings.

If $T \geq 2.5 \times 10^4$ °K. it may be seen from Table 5 that self absorption in the Lyman continuum will be small and so the intensity of this radiation inside the chromosphere may be taken equal to that escaping from the top, which is given by equation (5).

When T is appreciably less than 2.5×10^4 °K., the optical depth becomes much greater than unity and so the intensity J_ν will be approximately equal to $4\pi B_\nu$, where B_ν is defined as the ratio of the total emission coefficient to the absorption coefficient and for the Lyman continuum is given by (cf. Giovanelli 1949, equation (20))

$$B_\nu = \frac{6.1 \times 10^{-63} N_e^2 \nu^3 \exp(E_1^i - h\nu)/kT}{N_1 T^{3/2}}. \quad \dots (6)$$

Assuming for simplicity that the function $f(a) = 1 - (1+a)e^{-a} - a^2 \text{Ei}(-a)$ of equation (5) is independent of frequency, which introduces no great error, and substituting numerical values we find that

$$\Lambda_c = \frac{1}{N_1} \int_{\nu_o}^\infty \frac{J_\nu \alpha_\nu d\nu}{h\nu} = 1.19 \times 10^9 J_o [b + 2b^2 + b^3], \quad \dots (7)$$

for $T \geq 2.5 \times 10^4$ °K., where $b = kT/h\nu_o$ and J_o is the intensity at the head of the Lyman continuum.

For $T < 2.5 \times 10^4$ °K., $J_\nu \sim 4\pi B_\nu$ inside the chromosphere, so that

$$\Lambda_c = \frac{3.25 \times 10^{-7} N_e^2}{N_1 T^{3/2}} \exp(E_1^i/kT) \{-\text{Ei}(-E_1^i/kT)\}.$$

Thus, since $E_1^i/kT \gg 1$ at these temperatures

$$\Lambda_c \simeq \frac{3.25 \times 10^{-7} N_e^2}{N_1 T^{3/2}} \cdot \frac{kT}{E_1^i}. \quad \dots (8)$$

Values of Λ_c obtained in this way are given in Table 6 for two values of the electron concentration. For $T \geq 2.5 \times 10^4$ °K., where Λ_c is in general much less than BN_e , photoelectric ionization from the ground state may clearly be neglected.

At the lower temperatures, 1×10^4 and 1.5×10^4 °K., values of Λ_c obtained by using the approximate N_1 given in Table 4 are of the same order as the BN_e terms. We may find both Λ_c and N_1 in this case by combining equations (3) and (8). Ground state populations determined in this way are as follows :

T (°K.)	N_1
1×10^4	$6.09 \times 10^{-1} N_e$
1.5×10^4	$7.33 \times 10^{-3} N_e$

These values are little different from those of Table 4.

TABLE 6
COMPARATIVE VALUES OF Λ_c AND BN_e (SEE TEXT)

T (°K.)	Λ_c		BN_e
	$N_e = 5 \times 10^{11}$	$N_e = 10^{12}$	
1.0×10^4	0.0171	0.0342	$3.63 \times 10^{-13} N_e$
1.5×10^4	2.12	4.24	$2.13 \times 10^{-11} N_e$
2.5×10^4	16.4	64	$6.52 \times 10^{-10} N_e$
5.0×10^4	42	149	$9.65 \times 10^{-9} N_e$
1.0×10^5	110	364	$3.96 \times 10^{-8} N_e$
2.5×10^5	92	347	$8.67 \times 10^{-8} N_e$

(b) Effect of the Lyman Line Radiations

For $T \geq 5 \times 10^4$ °K. the ground state populations will be greater than those shown in Table 4, since the rate at which atoms are removed from this state by absorption of $L\alpha$ and $L\beta$ radiation is less than the rate of entry from the $3P$ and $2P$ states. We shall now compute N_1 in this case.

The intensity of Lyman line radiation at the base of the chromosphere may be seen from results of Giovanelli (1949) to be given approximately by :

$$J_\nu = \frac{4\pi\epsilon}{\alpha\lambda} \left[1 - \frac{2 \exp(-2\tau_1 \sqrt{3\lambda})}{1 + 2\sqrt{\lambda/3} + (1 - 2\sqrt{\lambda/3}) \exp(-2\tau_1 \sqrt{3\lambda})} \right], \quad \dots (9)$$

which may be written as

$$J_\nu = k(4\pi\epsilon/\alpha\lambda).$$

The values of Λ_α and Λ_β to be used in calculating the constants A and B of equation (3) should then be no greater than k times the values obtained by assuming the atmosphere to be optically thick to $L\alpha$ and $L\beta$.

Using Table 5, the approximate values of the k 's may be calculated, and are found to be given, for the line centres, by $k_\alpha \simeq k_\beta = 10^{-2}$ for $T = 10^5$ °K. and $k_\alpha \simeq k_\beta = 10^{-4}$ for $T = 2.5 \times 10^5$ °K.

Substituting the new values of Λ_α , Λ_β in the equations for N_1 we find

T ($^\circ\text{K}.$)	N_1
1×10^5	$3.50 \times 10^{-6} N_e$
2.5×10^5	$7.38 \times 10^{-7} N_e$

Although these values of N_1 will, in turn, modify the values of k , the resulting change in N_1 is insignificant.

TABLE 7
BASE STATE POPULATIONS FOR HYPOTHETICAL
CHROMOSPHERES (SEE TEXT)

T ($^\circ\text{K}.$)	N_1
1.0×10^4	$6.09 \times 10^{-1} N_e$
1.5×10^4	$7.33 \times 10^{-2} N_e$
2.5×10^4	$2.09 \times 10^{-4} N_e$
5.0×10^4	$8.78 \times 10^{-6} N_e$
	(or $2.0 \times 10^{-5} N_e$)
1.0×10^5	$3.50 \times 10^{-6} N_e$
2.5×10^5	$7.38 \times 10^{-7} N_e$

The values of N_1 adopted here for $N_e \leq 10^{12} \text{ cm.}^{-3}$ are set out in Table 7. These values include the effect of photoelectric ionization at low temperatures and of the small optical depth in the Lyman lines at high temperatures. The results should be correct to within a factor of about two.

For $T = 5 \times 10^4 \text{ }^\circ\text{K}.$ (where the optical depths in $L\alpha$ and $L\beta$ are about unity), the value of N_1 shown in brackets has been used for $N_e \leq 5 \times 10^{11} \text{ cm.}^{-3}$; this is the value obtained by application of the appropriate correction factors to Λ_α and Λ_β , as above.

VI. THE LYMAN CONTINUUM

The values of N_1 shown in Table 7 may be used, with specified values of N_0 , β , and temperature, to calculate J_ν from equation (5). These results, expressed in terms of the equivalent temperature for hemispherical radiation from a black body, are shown graphically in Figure 1. Giovanelli's value for $T = 2.5 \times 10^4 \text{ }^\circ\text{K}.$ and $N_0 = 10^{12} \text{ cm.}^{-3}$ is also plotted and it will be seen that the improved cross sections have not significantly affected the results.

Emission of Lyman continuous radiation reaches a maximum at a temperature of about $5 \times 10^4 \text{ }^\circ\text{K}.$ At high temperatures, where the atmosphere is effectively transparent, the emission depends only on recombination and so falls off as $T^{-\frac{1}{2}}$.

VII. THE LYMAN LINES

The intensity of the escaping radiation in the Lyman lines is given (Giovanelli 1949) by

$$J_\nu = \frac{4\pi\varepsilon}{\alpha\lambda} \left[1 - \frac{1 + \exp(-2\tau_1\sqrt{3\lambda})}{(1 + 2\sqrt{\lambda/3}) + (1 - 2\sqrt{\lambda/3}) \exp(-2\tau_1\sqrt{3\lambda})} \right]. \quad (10)$$

On substituting numerical values of ε/α and λ (estimated by the method used by Giovanelli (1949)) into (10), the central intensities of the Lyman lines shown in Figure 2 are obtained for $N_0 = 5 \times 10^{11}$ cm.⁻³, $\beta = 6 \times 10^{-9}$ cm.⁻¹. As

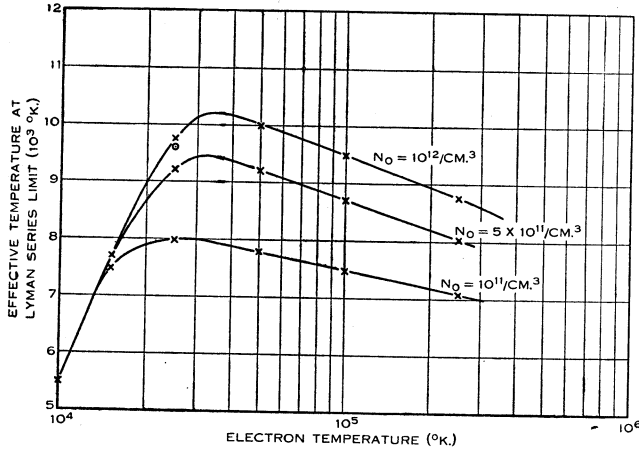


Fig. 1.—Effective temperature at the beginning of the Lyman continuum for $N_0 = 10^{11}$, 5×10^{11} , and 10^{12} cm.⁻³, $\beta = 6 \times 10^{-9}$ cm.⁻¹.

in the case of the Lyman continuum, the intensity of the emergent radiation passes through a maximum at $T \approx 5 \times 10^4$ °K.

The contour of a Lyman line may also be obtained from equation (10). Calculations show that λ does not vary very rapidly with electron temperature,

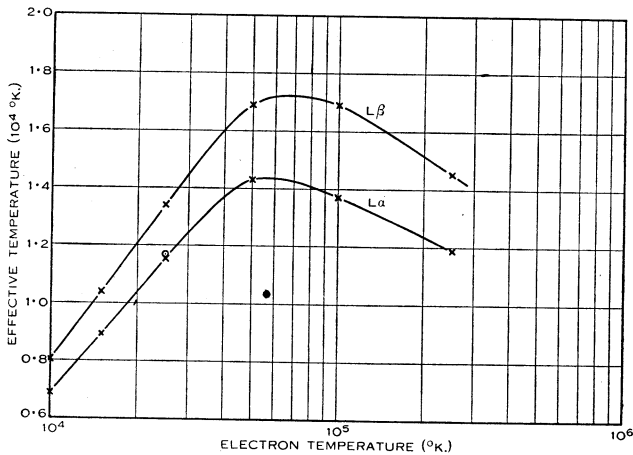


Fig. 2.—Effective temperature at the centre of $L\alpha$ and $L\beta$. $N_0 = 5 \times 10^{11}$ cm.⁻³, $\beta = 6 \times 10^{-9}$ cm.⁻¹.

and so the factor governing the intensity at a frequency of $\nu_0 \pm \Delta\nu$ is the optical depth, which takes the form $PN_0 \exp[-\gamma(\Delta\nu)^2]$, where P and γ are quantities which decrease with increasing T .

At the lower temperatures for which $\sqrt{3\lambda} \tau_1^\circ \gg 1$, the ratio $J_0/(4\pi\epsilon/\alpha\lambda)$ is effectively independent of T , and so the frequency at which this ratio is reduced to one-half will be such that $\sqrt{3\lambda} \tau_1$ is almost constant with T .

For high electron temperatures where $\sqrt{3\lambda} \tau_1^\circ \ll 1$, the profile of the emission line is undisturbed by self absorption, and is, at least not too far out in the wings, of the Doppler form. Consequently, at half-width, $\exp[-\gamma(\Delta\nu)^2] = \frac{1}{2}$, and since γ varies as T^{-1} , the half-width of the line varies as $T^{\frac{1}{2}}$. The term half-width is used for $L\alpha$ and $L\beta$ to denote the distance from the line centre at which the intensity has dropped to one-half of its value at the centre (our half-width is

TABLE 8
HALF-WIDTHS OF $L\alpha$ AND $L\beta$
 $N_0 = 5 \times 10^{11} \text{ cm.}^{-3}$, $\beta = 6 \times 10^{-9} \text{ cm.}^{-1}$

T (°K.)	$L\alpha$ (Å)	$L\beta$ (Å)
1.0×10^4	0.18	0.15 ₅
1.5×10^4	0.17	0.15
2.5×10^4	0.16	0.14
5.0×10^4	0.12	0.11
1.0×10^5	0.14	0.12
2.5×10^5	0.22	0.18

sometimes known as the "half-half-width"). The half-width increases with the value of the electron concentration at the base of the chromosphere—through the neutral atom concentration—for all temperatures, although the increase with N_0 may become negligible at high temperatures. The calculated half-widths, in Ångstrom units, for the $L\alpha$ and $L\beta$ lines are tabulated in Table 8 for $N_0 = 5 \times 10^{11} \text{ cm.}^{-3}$, $\beta = 6 \times 10^{-9} \text{ cm.}^{-1}$.

VIII. THE $H\alpha$ INTENSITY

Whereas the Lyman lines are of much greater intensity than the neighbouring continuous spectrum from the photosphere, the $H\alpha$ line appears dark against a brighter photospheric continuous spectrum. The computation of the $H\alpha$ contour is thus much more complicated, in that photospheric radiation cannot be ignored. The contour, which depends on the optical depth of the chromosphere, may be determined either by the chromosphere, by the photosphere, or, as is more probable, by a combination of both. In general, the chromosphere exerts its maximum effect near the centre of the line, where its optical depth is greatest. In the far wings, where the chromosphere is transparent, the computation of the contour will need to take account of the change with wavelength of the photospheric absorption and scattering coefficients.

In investigating these matters, we do not propose to consider in detail the

variations in physical conditions with optical depth. It is sufficient to assume, in the photosphere, B_v to be constant, and that the scattering parameter λ_v' does not change with optical depth. In the chromosphere we again take $4\pi\varepsilon/\alpha\lambda$ and λ to be constant both with frequency and with optical depth. The approximate solution of the equation of radiative transfer then becomes

$$J_c = \frac{4\pi\varepsilon}{\alpha\lambda} + a \exp(\sqrt{3\lambda}\tau) + b \exp(-\sqrt{3\lambda}\tau). \quad \dots\dots (11)$$

in the chromosphere, and

$$J_p = 4\pi B_v + \gamma \exp(-\sqrt{3\lambda'}\tau') \quad \dots\dots\dots (12)$$

in the photosphere, a , b , and γ being integration constants and τ and τ' being optical depths measured from the top of the chromosphere and photosphere respectively. For the sake of clarity, frequency subscripts have been omitted.

To obtain the required intensity of the radiation in the chromosphere we make use of the boundary conditions that (i) across the interface of the two atmospheres the intensities and fluxes are continuous, and (ii) at the outer boundary of the chromosphere there is no incident radiation. These conditions are equivalent respectively to

$$J_c = J_p, \quad \frac{\partial J_c}{\partial \tau} = \frac{\partial J_p}{\partial \tau}$$

at the interface, and

$$\frac{2}{3} \frac{\partial J_c}{\partial \tau} = J_c \text{ at } \tau = 0.$$

With these conditions we find that

$$a = -\frac{4\pi\varepsilon/\alpha\lambda + (1 + 2\sqrt{\lambda/3})b}{1 - 2\sqrt{\lambda/3}}, \quad \dots\dots\dots (13)$$

$$a = -\frac{\sqrt{\lambda'}(4\pi\varepsilon/\alpha\lambda - 4\pi B_0) + b(\sqrt{\lambda'} - \sqrt{\lambda}) \exp(-\sqrt{3\lambda}\tau_1)}{(\sqrt{\lambda} + \sqrt{\lambda'}) \exp(\sqrt{3\lambda}\tau_1)}, \quad \dots\dots\dots (14)$$

where τ_1 is the total optical depth of the chromosphere and B_0 is the value of B_v at the top of the photosphere.

At the outer boundary $J_c = 4\pi\varepsilon/\alpha\lambda + a + b$. Substituting values of a and b found from the solutions of the equations (13) and (14), we find that the emergent intensity is given by

$$J_c = J_0 + J_1, \quad \dots\dots\dots (15)$$

where

$$J_0 = \frac{4\pi\varepsilon}{\alpha\lambda} \left[1 - \frac{\sqrt{\lambda} + \sqrt{\lambda'} + (\sqrt{\lambda} - \sqrt{\lambda'}) \exp(-2\tau_1\sqrt{3\lambda})}{(1 + 2\sqrt{\lambda/3})(\sqrt{\lambda} + \sqrt{\lambda'}) + (1 - 2\sqrt{\lambda/3})(\sqrt{\lambda} - \sqrt{\lambda'}) \exp(-2\tau_1\sqrt{3\lambda})} \right]$$

and

$$J_1 = -\frac{4\sqrt{\lambda/3}\sqrt{\lambda'} \exp(-\sqrt{3\lambda}\tau_1)[4\pi\varepsilon/\alpha\lambda - 4\pi B_0]}{(1 + 2\sqrt{\lambda/3})(\sqrt{\lambda} + \sqrt{\lambda'}) + (1 - 2\sqrt{\lambda/3})(\sqrt{\lambda} - \sqrt{\lambda'}) \exp(-2\tau_1\sqrt{3\lambda})}$$

In estimating the value of B_0 in (15), we may note that over the wavelength range concerned, B_0 is independent of frequency. In the far wings of $H\alpha$, where τ tends to zero,

$$J_c = \frac{2\sqrt{\lambda'/3}}{1+2\sqrt{\lambda'/3}} \times 4\pi B_0.$$

Since, as will be shown later, $\lambda'=1$ here,

$$J_c = \frac{4\pi B_0}{1+\sqrt{3}/2} \dots\dots\dots (16)$$

This, however, represents the emergent continuous radiation which for the case of the Sun at $H\alpha$ approximates to the hemispherical radiation from a black body at 6150 °K. Denoting this by J_w , we have, from (16),

$$4\pi B_0 = (1 + \sqrt{3}/2)J_w \dots\dots\dots (17)$$

Finally, substituting for $4\pi B_0$ from this equation into equation (15) we find

$$J_c = \frac{4\pi\varepsilon}{\alpha\lambda} \left[\frac{1 - (\sqrt{\lambda} + \sqrt{\lambda'}) + 4\sqrt{\lambda\lambda'}/3 \exp(-\sqrt{3\lambda}\tau_1) + (\sqrt{\lambda} - \sqrt{\lambda'}) \exp(-2\tau_1\sqrt{3\lambda})}{D} \right] + \frac{2(1+2/\sqrt{3})\sqrt{\lambda\lambda'} \exp(-\sqrt{3\lambda}\tau_1)J_w}{D} \dots\dots\dots (18)$$

where

$$D = (1 + 2\sqrt{\lambda/3})(\sqrt{\lambda} + \sqrt{\lambda'}) + (1 - 2\sqrt{\lambda/3})(\sqrt{\lambda} - \sqrt{\lambda'}) \exp(-2\tau_1\sqrt{3\lambda}).$$

We shall now consider the evaluation of ε/α and of λ and λ' in equation (18).

(a) *The Ratio ε/α*

The ratio ε/α depends to some extent on the $H\alpha$ intensity, a lower intensity allowing a higher population in the metastable $2S$ state. Consequently the evaluation of ε/α and α from the equilibrium equation must be in terms not only of atomic constants, but also of the rate of absorption of $H\alpha$ quanta by atoms in the $2S$ state, which may be written

$$\Lambda_{2S-3P} N_{2S} = \int \frac{J_\nu \alpha_\nu d\nu}{h\nu} \dots\dots\dots (19)$$

Since the maximum value of α_ν occurs at the centre of the line, and J_ν varies less rapidly with ν than does α_ν , the integral is given quite closely by $(J_0/h\nu_0) \int \alpha_\nu d\nu$ where J_0 is the intensity at the centre of the line.

The emergent radiation at the centre of the line comes, on the average, from regions where $\sqrt{3\lambda}\tau^\circ = 1$, and a study of conditions at this level enables ε/α , and consequently the $H\alpha$ intensity, to be estimated. The approximate electron concentration at this level has been obtained by assuming a suitable value for the $H\alpha$ intensity—in the case of the Sun this corresponds approximately to that inside a black body at 5000 °K.—calculating $\sqrt{3\lambda}\tau^\circ$ in terms of N_e , and finding N_e for $\sqrt{3\lambda}\tau^\circ = 1$. For $\sqrt{3\lambda}\tau_1^\circ < 1$ the values of ε/α and α have been computed for the electron concentration at the base of the chromosphere.

(b) *The Scattering Parameters*

The photospheric scattering parameter λ' is defined by the equation

$$1 - \lambda'_v = \frac{\sigma_v}{\sigma_v + \kappa_v + \kappa_0}, \dots\dots\dots (20)$$

where σ_v and κ_v are the coefficients of scattering and "true" absorption for the H α line, and κ_0 is the coefficient of continuous absorption by negative hydrogen ions, at the frequency ν . Values of κ_0 may be obtained from tables given by Chandrasekhar and Breen (1946). To evaluate λ'_v we make use of λ_L , the line scattering parameter defined by the equation

$$1 - \lambda_L = \frac{\sigma_v}{\sigma_v + \kappa_v}. \dots\dots\dots (21)$$

Then from equation (20)

$$\begin{aligned} \lambda'_v &= \frac{\sigma_v + \kappa_v}{\sigma_v + \kappa_v + \kappa_0} \lambda_L + \frac{\kappa_0}{\sigma_v + \kappa_v + \kappa_0} \\ &= \frac{\alpha_v \lambda_L}{\alpha_v + \kappa_0} + \frac{\kappa_0}{\alpha_v + \kappa_0}, \dots\dots\dots (22) \end{aligned}$$

as $\sigma_v + \kappa_v = \alpha_v$. We see at once that, as $\alpha_v \rightarrow 0$, $\lambda'_v \rightarrow 1$.

To estimate λ_L we make use of the result obtained by calculation that the H α scattering parameter in the chromosphere has a value (about 0.35) which is relatively insensitive to variations in N_e or T ; for the high rate of spontaneous $3P \rightarrow 1S$ transition, which is independent of the physical conditions, determines its magnitude. For higher N_e , collision transitions from the 3-quantum state would become increasingly more frequent and λ approach unity. Thus λ_L will differ from λ only if collision transitions from the 3 states are much more important in the photosphere than in the chromosphere.

Using cross-section data based on general theorems due to Bohr, Peierls, and Placzek (1949) for low energy inelastic collisions, it may be readily shown that, in the photosphere, transitions from the $3P$ state are still predominantly spontaneous provided the electron concentration does not much exceed 10^{13} cm.⁻³. In the layers responsible for the radiation in the wings of H α , however, N_e may exceed this value, and it is a little difficult to see what λ_L will be. It is possible, however, to obtain its value in the wings from observation, as shown later, and as this also turns out to be about 0.35, it presumably applies closer to the line centre, where collision transitions will be of less importance.

In the wings of H α the optical depth of the chromosphere is effectively zero, and the emergent intensity can be obtained by substituting $\tau_1 = 0$ in equation (18), when we find

$$\frac{J_v}{J_w} = 1.866 \frac{2\sqrt{\lambda'_v/3}}{1 + 2\sqrt{\lambda'_v/3}}, \dots\dots\dots (23)$$

Hence

$$\lambda'_v = \frac{3}{4} \left[\frac{r_v}{1.866 - r_v} \right]^2, \dots\dots\dots (24)$$

where $r_v = J_v/J_w$.

Far enough away from the line centre, the H α absorption coefficient may be written

$$\alpha_\nu = b/(\Delta\nu)^2, \dots\dots\dots (25)$$

where b is a function of N_{2S} , N_{2P} , and N_e . Its dependence on N_e arises from the Stark broadening of the energy levels, compared with which natural broadening may generally be neglected in the photosphere.

From (25) and (22) we find

$$\lambda_{\nu'} = \frac{\lambda_L + gx}{1 + gx},$$

or

$$\frac{1}{1 - \lambda_{\nu'}} = \frac{gx}{1 - \lambda_L} + \frac{1}{1 - \lambda_L}, \dots\dots\dots (26)$$

where $g = \kappa_0/b$ and $x = (\Delta\nu)^2$.

This relation may now be compared with observations of the contour of H α emitted by the sun.

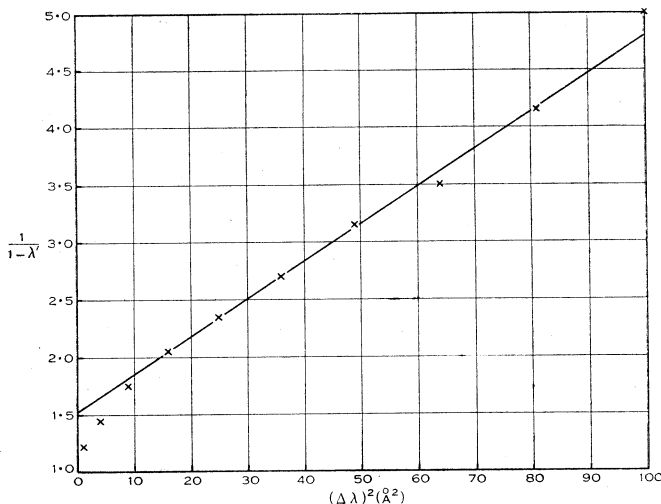


Fig. 3.—Graph of $1/(1 - \lambda')$ v. $(\Delta\lambda)^2$ for H α ; see text.

Figure 3 shows $1/(1 - \lambda_{\nu'})$, obtained from Evans's (1940) results via equation (24), plotted against $(\Delta\nu)^2$. From the linear nature of the graph it would appear that, beyond 4 Å from the centre of the line, the effective values of λ_L and κ_0/b are constant, being 0.35 and 4.3×10^{-24} sec.². Using data given by Chandrasekhar and Breen (1946) and well-known expressions for Stark broadening (see, e.g. White 1934), the ratio κ_0/b may be calculated, for a gas in thermodynamic equilibrium, in terms of $N_e (=N_+)$ and T . The value found above is numerically equal to that which would be obtained for an atmosphere in thermodynamic equilibrium at about 5700 °K. if the energy levels are Stark broadened and $N_e = 10^{12}$ cm.⁻³, and 6000 °K. if $N_e = 10^{13}$ cm.⁻³.

Equation (26) may be used to calculate $\lambda_{\nu'}$ from λ_L and g . It is clear that if the wing intensities are now computed from equation (23), they must fit

Evans's experimental results over the region of wavelengths where the curve of Figure 3 is linear.

Evans's results from the H α contour were used in plotting Figure 3, since they provide data at a large number of wavelengths. The photospheric parameters have been also computed from the means of four sets of observations

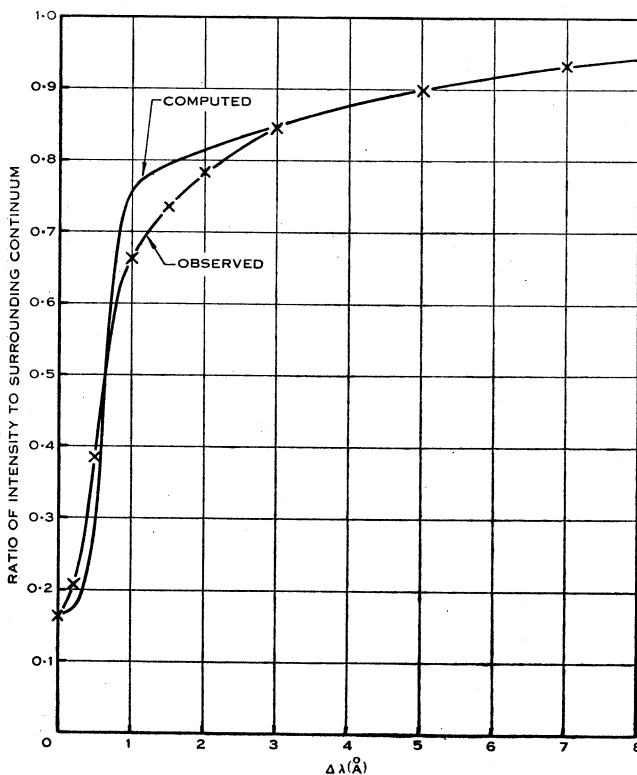


Fig. 4.—H α contour calculated for $T=2.5 \times 10^4$ °K., $N_0=2 \times 10^{11}$ cm.⁻³, $\beta=6 \times 10^{-9}$ cm.⁻¹, compared with observational results.

(Minnaert 1927 ; Thackeray 1935 ; Evans 1940 ; ten Bruggencate *et al.* 1949), the resultant values of α_v and λ_L obtained being

$$\alpha_v = \frac{1.62 \times 10^{14}}{(\Delta v)^2},$$

$$\lambda_L = 0.37,$$

for

$$\kappa_0 = 10^{-9} \text{ cm.}^{-1}.$$

This value of λ_L is closely equal to the value computed for the chromosphere, so that λ_L may be taken to be constant for the whole line.

Figures 4 and 5 show H α contours computed from these data for $T=2.5 \times 10^4$ °K., $N_0=2 \times 10^{11}$ cm.⁻³, and $\beta=6 \times 10^{-9}$ cm.⁻¹. Figure 5 also shows the effect of an increased electron concentration at the base of the chromosphere. The shape of the line is clearly sensitive to N_0 .

Central intensities of the emergent H α line have been computed over the full range of temperatures, with the approximation $\lambda_{v_0}' = \lambda$. For a given electron concentration N_0 at the base of the chromosphere, the intensity depends,

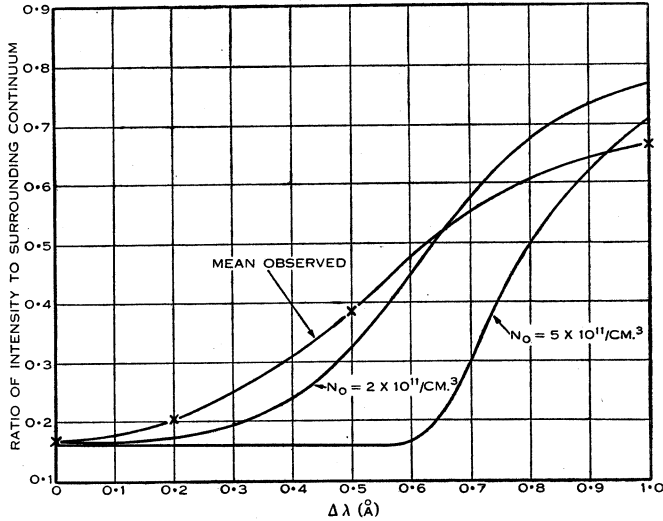


Fig. 5.—Contour of H α near the centre of the line calculated for $N_0 = 2 \times 10^{11}$ cm. $^{-3}$ and $N_0 = 5 \times 10^{11}$ cm. $^{-3}$ with $T = 2.5 \times 10^4$ °K., $\beta = 6 \times 10^{-9}$ cm. $^{-1}$.

through the optical depth, on the electron gradient β . Results of calculations are shown in Table 9 for $\beta = 6 \times 10^{-9}$ cm. $^{-1}$ and in Table 10 for an atmosphere in hydrostatic equilibrium. These tables show the contributions of the chromospheric and photospheric components to the central intensity of the emergent

TABLE 9
CONTRIBUTIONS OF CHROMOSPHERE AND PHOTOSPHERE TO H α CENTRAL INTENSITY
 $\beta = 6 \times 10^{-9}$ cm. $^{-1}$

T (°K.)	N_0 (cm. $^{-3}$)		5×10^{12}		10^{12}		5×10^{11}		10^{11}	
1.0×10^4	9	0	9	0	9	0	9	0	9	0
1.5×10^4	12	0	12	0	12	0	12	0	12	2
2.5×10^4	16	0	16	0	16	0	16	0	14	16
5.0×10^4	62	0	62	0	62	0	42	25	2	68
1.0×10^5	128	0	50	43	14	59	0	73	0	73
2.5×10^5	81	63	0	76	0	76	0	76	0	76

H α radiation in units such that the intensity of the surrounding continuum equals 100. The chromospheric component is shown on the left of each column. The total central intensity is given by the sum of the two components.

The central intensities depend upon the optical depths and for the lower temperatures, $T \leq 2.5 \times 10^4$ °K., should be fairly reliable. For $T > 2.5 \times 10^4$ °K., however, the optical depth is more difficult to estimate owing to the low value

TABLE 10
CONTRIBUTIONS OF CHROMOSPHERE AND PHOTOSPHERE TO H α CENTRAL INTENSITY
HYDROSTATIC EQUILIBRIUM

T (°K.)	N_0 (cm. ⁻³)	10 ¹²		5 × 10 ¹¹		10 ¹¹	
		1.0 × 10 ⁴	9	0	9	0	9
1.5 × 10 ⁴	12	0	12	0	12	2	
2.5 × 10 ⁴	16	0	16	0	14	16	
5.0 × 10 ⁴	30	0	30	0	9	61	
1.0 × 10 ⁵	68	0	41	28	0	73	
2.5 × 10 ⁵	30	62	2	73	0	76	

of $\sqrt{3\lambda\tau_1}$ in the Lyman lines, making the calculated ratios N_{3p}/N_{1s} and N_{2p}/N_{1s} somewhat uncertain. Nevertheless the errors in central intensity should not be very great, as the errors in photospheric and chromospheric contributions to some extent balance one another.

TABLE 11
CENTRAL INTENSITIES AND HALF-WIDTHS OF H α AT VARIOUS CHROMOSPHERIC
TEMPERATURES
 $N_0 = 5 \times 10^{11}$ cm.⁻³, $\beta = 6 \times 10^{-9}$ cm.⁻¹

T (°K.)	Central Intensity	Half-widths (Å)
1.0 × 10 ⁴	0.09	0.64
1.5 × 10 ⁴	0.12	0.71
2.5 × 10 ⁴	0.16	0.86
5.0 × 10 ⁴	0.67	~3
1.0 × 10 ⁵	0.73	~4
2.5 × 10 ⁵	0.76	~4
Observed	0.166	0.79

Half-widths of the emergent H α lines for various physical conditions may be calculated from a knowledge of the quantities occurring in (18) and are shown in Table 11, together with central intensities, for $N_0 = 5 \times 10^{11}$ cm.⁻³ and $\beta = 6 \times 10^{-9}$ cm.⁻¹.

When the optical depth in H α is very small, the emergent intensity will be given approximately by equation (23) which, from equation (26), represents a line of half-width about 4 Å, and central intensity about 0.75 J_w .

On the other hand, when the central intensity is relatively low the photospheric component contributes to the emergent radiation as soon as the chromospheric optical depth becomes small enough to allow it. In normal circumstances this occurs about 1 Å, or even less, from the centre and consequently the half-width in this case is controlled by both photosphere and chromosphere, being of the order of 0.5 Å. This accounts for the very great differences among the values of the half-widths shown in Table 11.

The mean central intensity and half-width from the above four sets of solar observations are given at the bottom of the corresponding column of Table 11. The agreement between observed values and those calculated for $T=2.5 \times 10^4$ °K. is probably only fortuitous, owing to the approximate methods involved in the calculations and the uncertainty in the data. It would seem, however, that observations are compatible with temperatures up to about 3.5×10^4 °K. in those regions of the chromosphere which give rise to the observed H α radiation.

IX. NON-COHERENT SCATTERING

The results obtained above for the contours and central intensities of the Lyman and H α lines are based explicitly on the assumption of coherent scattering whose intensity is independent of direction. We shall now obtain the form of the contour in L α and H α with a simple model of non-coherent scattering whose intensity is still uniform with angle. We assume that non-coherency is introduced by a Doppler shift in frequency associated with a Maxwellian velocity distribution at the kinetic temperature T , implying that the finite width of the line is due to thermal velocities alone. Doppler shifts are not uniformly distributed with angle, but for simplicity the angular variation is neglected. This should give reasonable results at frequencies not too far from the centre of the line.

With coherent scattering a quantum of frequency ν' which is absorbed and subsequently scattered is re-emitted with the same frequency. In the present case, however, the probability that the frequency of the scattered quantum will lie between ν and $\nu+d\nu$ is given by

$$p(\nu)d\nu = \sqrt{\gamma/\pi} \exp[-\gamma(\nu-\nu_0)^2]d\nu, \dots\dots\dots (27)$$

where

$$\gamma = \sqrt{\frac{M}{2kT}} \frac{c}{\nu_0},$$

M being the mass of the hydrogen atom. Then the total energy emitted per second from unit volume into unit solid angle per unit frequency range is

$$E_\nu = \frac{(1-\lambda)\sqrt{\gamma/\pi} \exp[-\gamma(\nu-\nu_0)^2] \int_0^\infty J_{\nu'} \alpha_{\nu'} d\nu'}{4\pi} + \epsilon_\nu, \dots\dots\dots (28)$$

where ϵ_ν is the "true" emission of the medium.

For simplicity we take $J_{\nu'}$ to be constant for all frequencies and equal to J_0 , the value at the centre of the line, an assumption which makes little difference to the value of the integral.

Since $\alpha_\nu = \alpha_0 \exp[-\gamma(\nu - \nu_0)^2]$ over the region of Doppler absorption, it follows that equation (28) then becomes

$$E_\nu = \frac{(1-\lambda) \exp[-\gamma(\nu - \nu_0)^2] J_0 \alpha_0}{4\pi} + \epsilon_\nu, \dots\dots (29)$$

and

$$B_\nu = \frac{E_\nu}{\alpha_\nu} = \frac{(1-\lambda) J_0}{4\pi} + \frac{\epsilon_\nu}{\alpha_\nu} \dots\dots\dots (30)$$

Making use of Eddington's approximation we may write the equation of radiative transfer in the form (see, e.g. Rosseland 1936)

$$\frac{1}{3} \frac{\partial^2 J_\nu}{\partial \tau_\nu^2} = J_\nu - 4\pi B_\nu, \dots\dots\dots (31)$$

which by equation (36) gives

$$\frac{1}{3} \frac{\partial^2 J_\nu}{\partial \tau_\nu^2} = J_\nu - (1-\lambda) J_0 - \frac{4\pi \epsilon_\nu}{\alpha_\nu} \dots\dots\dots (32)$$

Assuming, as before, that λ is uniform throughout the atmosphere, and that $4\pi\epsilon/\alpha\lambda$ is constant or varies only linearly with optical depth, the solution of equation (32) for the central intensity is

$$J_0 = \frac{4\pi\epsilon}{\alpha\lambda} + a \exp(\sqrt{3\lambda}\tau) + b \exp(-\sqrt{3\lambda}\tau), \dots\dots\dots (33)$$

where subscripts in ν_0 have been omitted on the right-hand side.

Substituting J_0 from (33) we find

$$\frac{1}{3} \frac{\partial^2 J_\nu}{\partial \tau_\nu^2} = J_\nu - \frac{4\pi\epsilon}{\alpha\lambda} - (1-\lambda)[a \exp(\sqrt{3\lambda}k\tau_\nu) + b \exp(-\sqrt{3\lambda}k\tau_\nu)], \dots\dots\dots (34)$$

where $\tau_0 = k\tau_\nu$, that is, $k = \exp \gamma(\nu - \nu_0)^2$.

The solution of (34) follows simply, giving

$$J_\nu = \frac{4\pi\epsilon}{\alpha\lambda} + A \exp(\sqrt{3}\tau_\nu) + B \exp(-\sqrt{3}\tau_\nu) + \frac{1-\lambda}{1-\lambda k^2} [a \exp(\sqrt{3\lambda}k\tau_\nu) + b \exp(-\sqrt{3\lambda}k\tau_\nu)]. \dots\dots\dots (35)$$

The relevant boundary conditions are the same as in the case of coherent scattering and are applicable to each frequency. For Lyman line radiation, evaluation of the constants a , b , A , and B gives the following expression for the emergent intensity

$$\frac{J_\nu}{4\pi\epsilon/\alpha\lambda} = 1 - R_1 - R_2, \dots\dots\dots (36)$$

where

$$R_1 = [1 + \exp(-2\tau_1 \nu \sqrt{3})] \times \left[\frac{1 - \lambda \left\{ \frac{1 + 2k\sqrt{\lambda/3} + (1 - 2k\sqrt{\lambda/3}) \exp(-2\tau_1 \nu \sqrt{3\lambda})}{1 - \lambda k^2} \left(\frac{1 + 2\sqrt{\lambda/3} + (1 - 2\sqrt{\lambda/3}) \exp(-2\tau_1 \nu \sqrt{3\lambda})}{1 + 2/\sqrt{3} + (1 - 2/\sqrt{3}) \exp(-2\tau_1 \nu \sqrt{3})} \right) \right\}}{1 + 2/\sqrt{3} + (1 - 2/\sqrt{3}) \exp(-2\tau_1 \nu \sqrt{3})} \right]$$

and

$$R_2 = \frac{1-\lambda}{1-\lambda k^2} \left[\frac{1 + \exp(-2\tau_1 \nu \sqrt{3\lambda})}{1 + 2\sqrt{\lambda/3} + (1 - 2\sqrt{\lambda/3}) \exp(-2\tau_1 \nu \sqrt{3\lambda})} \right].$$

For $H\alpha$, the expression for J_ν is very unwieldy but follows in a straightforward manner on application of the boundary conditions.

The $L\alpha$ and $H\alpha$ intensities at various distances from the line centres are shown in Tables 12 and 13. The calculations are made for an atmosphere with $T=2.5 \times 10^4$ °K. and $\beta=6 \times 10^{-9}$ cm.⁻¹. $N_0=5 \times 10^{11}$ cm.⁻³ for $L\alpha$ and

TABLE 12
EMERGENT INTENSITY ACROSS $L\alpha$
 $T=2.5 \times 10^4$ °K., $\beta=6 \times 10^{-9}$ cm.⁻¹, $N_0=5 \times 10^{11}$ cm.⁻³

$\Delta\lambda$ (Å)	Non-coherent Scattering	Coherent Scattering
0	0.018	0.018
0.05	0.022	0.018
0.10	0.041	0.018
0.15	0.156	0.011
0.17	0.298	0.004
0.20	0.442	0.001
0.225	0.419	0
0.25	0.149	0
0.275	0.025	0
0.30	0.002	0

2×10^{11} cm.⁻³ for $H\alpha$. The double entries in the second and third columns of Table 13 represent the chromospheric (left) and photospheric (right) components of the emergent radiation. With $H\alpha$, non-coherent scattering over a Doppler

TABLE 13
EMERGENT INTENSITY NEAR THE CENTRE OF $H\alpha$
 $T=2.5 \times 10^4$ °K., $\beta=6 \times 10^{-9}$ cm.⁻¹, $N_0=2 \times 10^{11}$ cm.⁻³

$\Delta\lambda$ (Å)	Non-coherent Scattering		Coherent Scattering	
0	0.158	0.008	0.158	0.008
0.14	0.161	0.009	0.158	0.012
0.29	0.166	0.019	0.152	0.038
0.43	0.164	0.072	0.133	0.127
0.57	0.136	0.266	0.092	0.320

profile is assumed in both the chromosphere and photosphere. This restriction—to a Doppler profile—means that we are only able to compare the profiles near the centre of the line as the two cases are clearly not comparable in the wings. It will be seen that the contour of the Lyman line is considerably affected by the introduction of non-coherent scattering; the $H\alpha$ contours are practically

identical for coherent and non-coherent scattering in the particular case considered.

With the Lyman lines, the introduction of non-coherent scattering results in a broadening, and formation of an M-shaped contour in the emergent line, as may be seen from Table 12. The contours at the base of the atmosphere are similar for both types of scattering, each being flat-topped. The non-coherent profile is, however, still the broader of the two. It is clear that the computed central intensities of all lines will be the same as those obtained on the assumption of coherent scattering since, by replacing J_ν with J_0 in the integral of equation (34), we have recovered the equation of radiative transfer for the case of coherent scattering.

The very great difference in behaviour between the $L\alpha$ and $H\alpha$ contours for coherent and non-coherent scattering is due primarily to the differences in τ for the two lines. In the case considered, the absorption coefficient for $L\alpha$ radiation is of the order of 100 times that for $H\alpha$, at the centre of the lines. $L\alpha$ quanta are virtually trapped at the centre of the line, but may escape freely in the wings when their frequencies are redistributed by non-coherent scattering.

The variation of the shape of the contour with kinetic temperature may readily be seen. At temperatures greater than 5×10^4 °K., the optical depths in $H\alpha$ and $L\alpha$ for normal values of β and N_0 are so small that chromospheric scattering is unimportant. At temperatures below 5×10^4 °K., non-coherent scattering broadens the contour, the M-shaped profile appearing when the optical depth becomes fairly large.

X. DISCUSSION

It is rather difficult to see to what extent the results obtained in this paper may be applied to the Sun. The only direct observational evidence which is available for check is the $H\alpha$ contour, in particular the central intensity and half-width. The computed values of these quantities are based on an approximate solution of the equation of radiative transfer, whose terms are calculated with reasonable values of N_e , variations of which do not in general greatly affect the computed central intensity.

In the absence of a detailed knowledge of the physical structure of the chromosphere it seems difficult to improve on the approximations, or to estimate the error involved. It seems, however, that on the models adopted here the results quoted for central intensities should be correct to rather better than a factor of 2 at the lower temperatures, and so we should be justified on the basis of the computed central intensities in saying that the kinetic temperature of the regions responsible for the observed $H\alpha$ radiation lies somewhere in the range below 3.5×10^4 °K.

It is possible to make some inferences on the chromospheric temperature from observations of the $H\alpha$ profile. The observed rapid initial increase in intensity as we move away from the centre of the line must almost certainly be attributed to the effect of photospheric radiation penetrating the chromosphere, rather than one due solely to variations in the composition of

the chromosphere, since calculations indicate that the quantity $4\pi\varepsilon/\alpha\lambda$ does not vary sufficiently with electron concentration for this latter effect to be significant. The most important parameter in determining the contour at a given electron temperature is the total optical depth, which in turn depends on N_0 , the electron concentration at the base. If this is large enough, the intensity of the emergent line will be effectively constant for some distance from the centre, as may be seen from Figure 5. The value of N_0 for $T=2.5 \times 10^4$ °K., which best fits the observations, is 2×10^{11} cm.⁻³, and this is the value adopted in Figures 4 and 5. For $T=10^4$ °K. and $N_0=2 \times 10^{11}$ cm.⁻³, $\sqrt{3\lambda\tau_1} \cong 30$. This is rather too large to allow the photosphere to contribute at all before $\lambda=0.5$ Å. For this temperature the central intensity is rather low, viz. 0.09, suggesting that, if it possesses a temperature in the range discussed here, i.e. 10^4 °K. or more, the H α -emitting region of the chromosphere has a temperature of at least 1.5×10^4 °K.

XI. ACKNOWLEDGMENTS

The author wishes to express his thanks to Dr. D. R. Bates for making available the collision cross sections, and to Dr. R. G. Giovanelli for suggesting the investigation and for helpful discussions, both on the subject matter and during the course of the preparation of the paper.

XII. REFERENCES

- BATES, D. R., FUNDAMINSKY, A., LEECH, J. W., and MASSEY, H. S. W. (1950).—*Phil. Trans.* **243**: 93.
- BOHR, N., PEIERLS, R., and PLACZEK, G. (1949).—Quoted by Mott, N. F., and Massey, H. S. W. (1949).—“The Theory of Atomic Collisions.” 2nd Ed. p. 135. (Oxford Univ. Press.)
- TEN BRUGGENCATE, P., GOLLNOW, H., GUNTHER, S., and STROHMEIER, W. (1949).—*Z. Astrophys.* **26**: 51.
- CHANDRASEKHAR, S., and BREEN, F. H. (1946).—*Astrophys. J.* **104**: 430.
- EVANS, D. S. (1940).—*Mon. Not. R. Astr. Soc.* **100**: 156.
- GIOVANELLI, R. G. (1949).—*Mon. Not. R. Astr. Soc.* **109**: 298.
- MINNAERT, M. (1927).—*Z. Phys.* **45**: 610.
- MİYAMOTO, S. (1951a).—*Publ. Astr. Soc. Japan* **2**: 102.
- MİYAMOTO, S. (1951b).—*Publ. Astr. Soc. Japan* **2**: 113.
- PURCELL, E. M. (1952).—*Astrophys. J.* (in press).
- ROSSELAND, S. (1936).—“Theoretical Astrophysics.” p. 112. (Oxford Univ. Press.)
- THACKERAY, A. D. (1935).—*Mon. Not. R. Astr. Soc.* **95**: 293.
- THOMAS, R. N. (1948).—*Astrophys. J.* **108**: 142.
- THOMAS, R. N. (1949).—*Astrophys. J.* **109**: 480.
- UNSOLD, A. (1938).—“Physik der Sternatmosphären.” p. 189. (J. Springer: Berlin.)
- WHITE, H. E. (1934).—“Introduction to Atomic Spectra.” p. 435. (McGraw-Hill: New York.)